Available online at www.sciencedirect.com
SCIENCE DIRECT®
Applied Surface Science 222 (2004) 148–165
applied surface science
www.elsevier.com/locate/apsusc

Surface characterisation of electrografted random poly[carbazole-co-3-methylthiophene] copolymers on carbon fiber: XPS, AFM and Raman spectroscopy

A. Sezai Sarac[a,b,*,1], Syed A.M. Tofail[a], Marina Serantoni[a], John Henry[a], Vincent J. Cunnane[a], James B. McMonagle[a]

[a]*Istanbul Technical University, Department of Chemistry, 80626 Maslak, Istanbul, Turkey*
[b]*Materials and Surface Science Institute (MSSI), University of Limerick, Plassey Technological Park, Limerick, Ireland*

Received 13 June 2003; received in revised form 7 August 2003; accepted 7 August 2003

Abstract

Surface characterizations of thin film coatings of carbazole containing random poly(carbazole-co-3-methylthiophene) P[Cz-co-3-MeTh] copolymers on carbon fiber were performed. Coatings with different initial feed ratios of comonomers were electrochemically formed (grafted) onto carbon fibers by constant current electrolysis. The resulting copolymers were characterised with scanning electron microscopy (SEM), atomic force microscopy (AFM), X-ray photoelectron spectroscopy (XPS) and Raman spectroscopy. The characterization of the thin copolymer films was performed on the surface of the carbon fiber. This allows the relationship between the initial feed ratio of the comonomer, the resulting morphology and the surface structure of these thin film coatings to be investigated. The range of thickness increase (diameter) was from 200 nm to 6.74 μm depending on the polymer and copolymers used.

Keywords: Random conductive copolymers; Carbon fiber; AFM; XPS; Raman spectroscopy

1. Introduction

High performance carbon fibers can be combined with thermoset and thermoplastic resin systems. Polyacrylonitrile (PAN) based carbon fibers are under continual development and are used in composites in order to produce materials of lower density and greater strength. They are used for weaving, braiding, filament winding applications, unidirectional tapes and as prepreg tow for fiber placement having excellent creep, fatigue resistance, high tensile strength and stiffness characteristics.

The application of a polymeric/copolymeric 'interface', acting as a coupling agent, can improve the interfacial properties between reinforcing (carbon) fibers and the polymeric matrix [1–3]. However, these interfacial reactive groups need to be strongly bound to the carbon surface so that these copolymer materials can survive other subsequent treatments, i.e., treatment with thermoset thermoplastic resin systems

* Corresponding author. Tel.: +353-61-234174; fax: +353-61-213529.
E-mail address: sarac@itu.edu.tr (A.S. Sarac).
URL: http://www.atlas.cc.itu.edu.tr/∼sarac/.
[1] Tel.: +90-212-2853153; fax: +90-212-2856386.

0169-4332/$ – see front matter
doi:10.1016/j.apsusc.2003.08.008

or for the immobilization of enzymes (for biosensor microelectrode fabrication). The surfaces of these systems can also be reacted with metal catalysts, which bind strongly to the carbon fiber due to the presence of suitable functional groups in the conductive copolymer coating. For these reasons, the detailed characterization of strongly bound polymers or copolymers, having a homogeneous thin film, is important. Electrografting of copolymers with conductive and nonconductive contents onto carbon fibers were studied recently [4–9] (and references therein). These investigations have shown that the conductive copolymer coating of carbon fiber is indeed achievable.

The electropolymerization procedure of these copolymers offers the advantage of controlling the thickness and functionality of such a 'reactive' coating through selective processing parameters (i.e., the current density, monomer concentration, temperature, etc.) and uniform coatings are achieved. The inclusion of various functional groups opens the possibility of the use of such modified reinforcing fibers in the design and production of advanced reinforced polymeric composite materials. An electrografted polymeric 'coating' on carbon fibers can be superior to other composite based materials because of its continuous and homogeneous character, through the inclusion of various functional surface groups.

Polycarbazole is a functional polymer material suitable for electrografting applications on carbon fibers. Polycarbazoles have a fused planar structure and are insoluble and infusible, making them essentially impossible to process into flexible films or shaped objects. Alkylated polythiophene derivatives, i.e., polyalkythiophenes, show good environmental stability. Monosubstitution of thiophene at the 3-position of the ring introduces asymmetry to the monomer and subsequently allows regioisomerism in the polymer to occur. Thin films of regioregular HT-coupled polyalkythiophenes (head–tail) can have high conductivities. Therefore, the understanding of and the attainment of the underpinning science of these copolymers coatings can simultaneously broaden and allow better control over the properties of resulting material applications.

Owing to the unique physical properties of polyconjugated soluble polymers, they are currently receiving considerable attention. Among the aims of such studies have been improved elucidation of their structure–property relationships and assessing a wide variety of potential technological applications, i.e., electrocatalysis, fuel cell electrodes, biosensor microelectrodes, reinforced composites and biomedical applications.

In a previous study, some ter-arenes based on *N*-ethylcarbazole and thiophene were synthesised and polymerised [10]. *N*-ethylcarbazole was chosen as an internal conjugated moiety so as to provide a planar, synthetically flexible core, which could easily be derivatized with no loss in extent of conjugation [11].

In this study we report in detail the application and results of a number of surface characterization techniques, i.e., atomic force microscopy (AFM), X-ray photoelectron spectroscopy (XPS) and Raman spectroscopy, of several random copolymers on carbon fiber. The copolymer compositions produced are electrochemically polymerised onto carbon fiber [12] (the diameter of untreated carbon fiber is approximately 5.6 μm). Surface characterisation techniques were applied to the proposed structure of poly(3-methylthiophene) and the copolymer of carbazole-co-3-methylthiophene, as shown in Figs. 1 and 2. The effect of the type of monomer unit under various electrochemical deposition conditions and environments on the resulting electrografted copolymer carbon fibres, the effectiveness of these electrografting methods on the nanometre to micron scale and the relationship between the surface composition and morphological results were investigated.

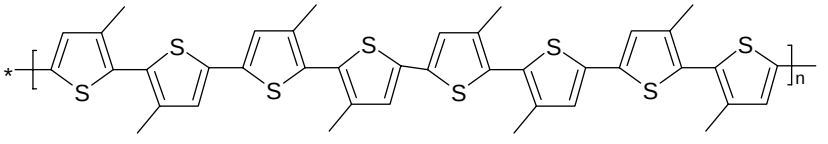

Fig. 1. Possible structure of poly(3-methylthiophene) (lines are indicating the methyl group).

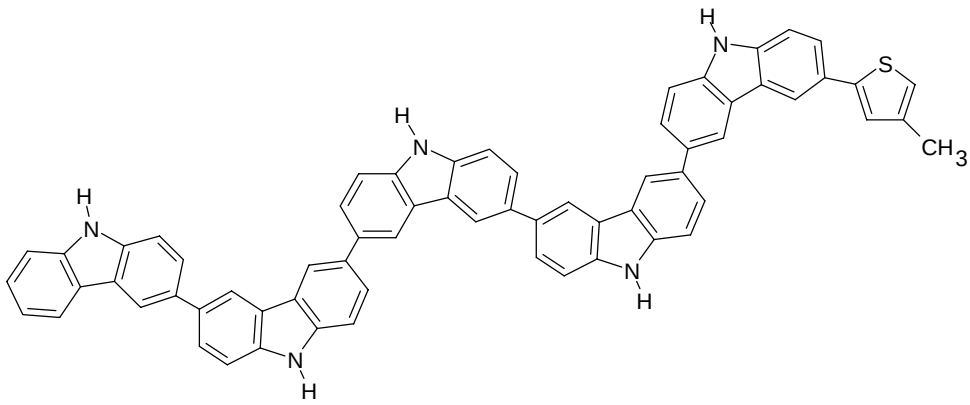

P[Cz-co-3MeTh]

Fig. 2. Proposed structure of carbazole-co-3-methylthiophene copolymer (S6).

2. Experimental

2.1. Materials

Polyacrylonitrile based carbon fiber (Hexcel AS4C, 12K carbon fibers having 12,000 single filaments in a roving) was used for this study. The monomers of carbazole (Cz), and 3-methylthiophene (3-MeTh) were supplied from Merck (synthesis grade) and tetramethylammonium perchlorate (TMAP) was supplied by Fluka (>99%) as the supporting electrolyte. All these chemicals were used without further purification.

2.2. Preparative electrochemical cell (constant current electrolysis)

The electrochemical cell used for the preparative electrocopolymerization procedure was a cylindrical shaped glass cell (50 mm in diameter by 70 mm in height) with an effective volume of approximately 100 ml. The carbon fibers were placed in a glass tube against the stainless-steel plate (V2A) in such a way that the carbon fibers dipped into electrolyte by up to 60 mm (in order to adjust the current density while keeping the applied current constant). The surface area of the stainlesssteel cathode used was 28.6 cm^2 at a temperature of 40 °C. The area of the fiber electrodes was 160 cm^2 (dipped 60 mm into the liquid in the cell). The electrolyte solution was magnetically stirred during the electropolymerization process. As a power supply, a galvanometer was used with an adjustable current between 0 and 4 A and a voltage ranging from 0 to 75 V. A constant current electrolysis was applied by keeping the current density ($i = I/A$ [mA/cm^2]) constant by calculating the geometric surface area of the carbon fibers (fiber diameter $d_f \approx 5.6$ μm). After the electrolysis, the carbon fibers were washed thoroughly with water and distilled acetone and with tetrahydofuran (THF). Afterwards the fibers were dried overnight in a vacuum oven at 1 mbar and at a temperature of 50 °C.

2.3. Atomic force microscopy images of electrografted polymers on carbon fibers

The AFM images reported in this study were obtained using an Explorer™, Scanning Probe Microscope, (TopoMetrix-ThermoMicroscope-VEECO). In this analysis the non-contact mode was used. The tips used were high resonance frequency silicon tips (frequency range 354–409 kHz), with a 120 μm long cantilever, a tip of 3–6 μm base, 10–20 μm long and a 20 nm tip radius. The raw data collected was processed by the TopoMetrix SPMLab NT Version 5.0 using left shadowing. In order to perform AFM analysis the carbon fibers were attached to a piece of

silicon wafer using a thin layer of Tempfix Adhesive (Neubauer Chemikalien, Germany).

2.4. X-ray photoelectron spectroscopic study, XPS parameters

The X-ray photoelectron spectroscopic study was performed on the as-introduced samples using a Kratos Axis 165 spectrometer. A monochromatic AlK_α (energy = 1486.6 eV) radiation source with an energy resolution of 0.4 eV at pass energy of 20 eV was used with 15 mA current and 15 kV voltage. For peak synthesis, a Shirley type background was utilised.

2.5. Raman spectroscopy

Raman Spectroscopy was conducted on a DILOR XY Labram using a He–Ne 20 mW laser under a tension of 7.60 mA through an 1800 grating and the generated spectra were collected with a Peltier cooled CCD detector. An excitation source of 514.5 nm was used. Raman focusing and imaging was conducted using a confocal microscope (Olympus BX40) with an objective of X100. Other operation parameters applied were a pinhole of 250 μm, a slit opening of 150 μm, an accumulation time of 120 s and an accumulation number of 10. The XY stage was used to conduct line scans of the samples in order to investigate phase homogeneity of the copolymer surface layer on the Hexcel carbon fiber and to ensure that better compositional information was obtained.

3. Results and discussions

3.1. Materials

The successful electrografting of carbon fibers with polymer/copolymer coatings was achieved by electrocopolymerization onto Hexcel carbon fibers. The samples produced in this study, the feed ratio of the monomers applied, their concentration of monomer and their subsequent changes in weight (Δw) and change in radius (Δr) are given in Table 1.

All reactions were achieved in 120 min except for sample 4 (S4), which was electrocopolymerised in 20 min. The change in radius was obtained by dividing the difference in the average diameter of the grafted and ungrafted fiber (obtained by scanning electron microscopy (SEM) by a factor of two.

3.2. Surface analysis of electrografted copolymer on carbon fiber by XPS

The high-resolution XPS spectra for the untreated carbon fiber (sample S1) in the regions of C 1s, N 1s, O 1s and S 2p are shown in Fig. 3. The main C 1s peak shows a small amount of asymmetry on the higher binding energy side (Fig. 3a). There are also two shake-up satellite peaks present at approximately 293.4 and 296.1 eV. These satellite peaks are due to the $\pi \rightarrow \pi^*$ transition in the aromatic ring of the carbon fiber. The observed peak has been deconvoluted into three peaks. The main peak, denoted as *l* in Fig. 3a, appearing at 285 eV is attributed to the C–C bonding irrespective of the type of hybridisation.

Table 1
Increase in weight (Δw) and thickness (Δr) of P[Cz-co-MeTh], PCz and PMeTh coated fiber relative to ungrafted fiber

	Copolymer monomer	Feed ratio of $[Cz]_0/[MeTh]_0$	Initial concentration of monomers (M)		Δw (mg)	Δr (μm) [11]
			$[Cz]_0$	$[MeTh]_0$		
S1	Untreated carbon fiber	–			–	–
S2	Cz12		0.075		114.6	6.74
S3	MeTh13			0.213	0.4	–
S4	MeThCz11	0.35	0.075	0.211	37.7	0.73
S5	MeThCz6	0.36	0.057	0.157	96.7	0.20
S6	MeThCz7	0.66	0.050	0.075	85.0	3.75
S7	MeThCz8	1.85	0.100	0.054	142.8	–

The different feed ratio of comonomers on the electrocopolymerization of carbazole with 3-MeTh in 0.1 M TMAP/100 ml DMF at constant current electrolysis I = 100 mA are also outlined.

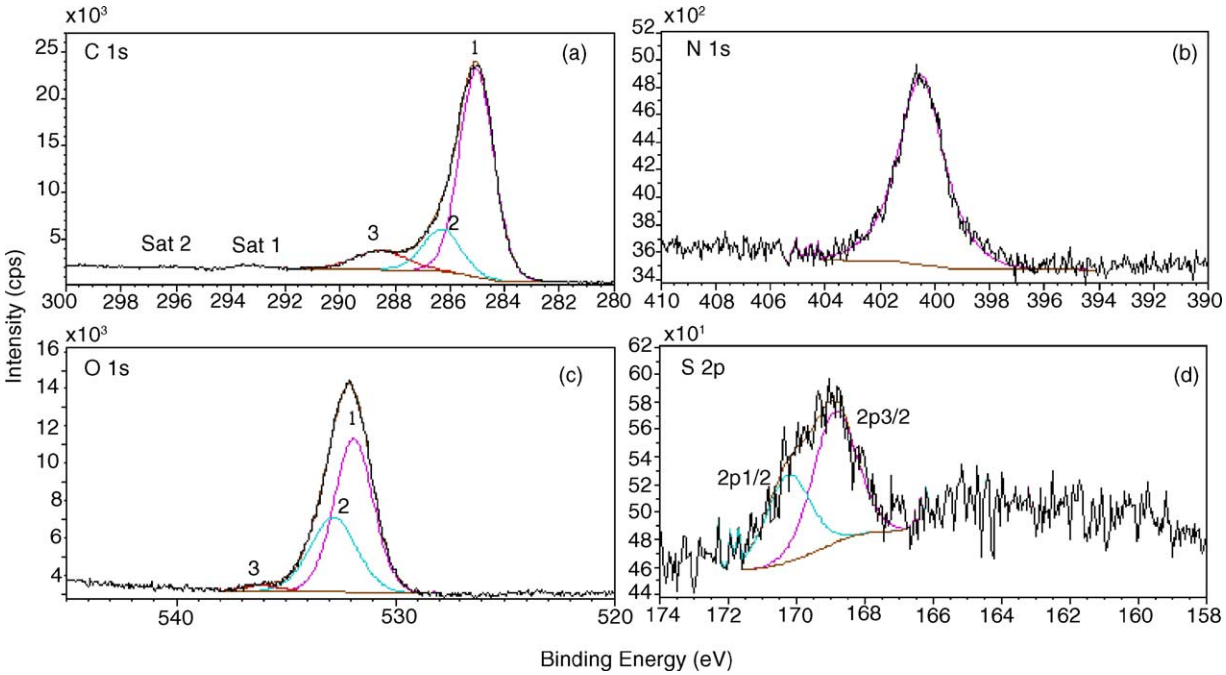

Fig. 3. C 1s (a); N 1s (b); O 1s (c) and S 2p (d) core-level XPS spectra of untreated carbon fiber.

The presence of asymmetry on the higher binding energy side indicates a second peak, denoted as 2 in Fig. 3a, observed at approximately 286.3 eV. This peak can be attributed to a combined contribution of C single bonded to both N and O. Nitrogen functionalities have a primary substituent effect which is markedly dependent on the nature of substitution. Thus, the C 1s XPS core-line shifts for $–N(CH_3)_2$, –NCO and $–NO_2$ functionalities are 0.2, 0.6, and 1.8, respectively [13]. As a general rule, oxygen induces a primary substitution effect on the C 1s core-line, which results in a shift on the higher binding energy side, of approximately 1.5 eV, for each C–O bond. Thus, O–C–O and C=O (double bonded oxygen) both give similar C 1s binding energies. The third peak, 3, in Fig. 3a is assigned to the carbonate and/or carboxylic functionalities.

The presence of N on the surface is quite significant as can be seen from the intensity of the N 1s spectrum in Fig. 3b. The energy position of the nitrogen (400.5 eV) is indicative of C–N bonding [14]. This peak has been assigned to as coming from the N-containing residues, perhaps due to the incomplete oxidation of the PAN source from which the fibres in questions are made. The O 1s binding energy due to organic functionalities falls within a narrow range in the region of 2 eV at approximately 533 eV. The singly bound oxygen has a higher binding energy than the doubly bonded O. The singly bound oxygen in carboxyl and carbonate groups appears at even higher binding energies. As a result of these chemical properties, the O1s peak for the untreated fibre has been deconvoluted into three components, denoted as 1, 2 and 3 in Fig. 3c, which are assigned to the C=O, C–O and CO_3/COOR functionalities, respectively. The S 2p spectrum (Fig. 3d) indicates the possibility of the presence of oxygenated sulphur. The shoulder at approximately 170.3 eV in the S 2p peak is due to spin orbit splitting of the S 2p peak into a S $2p_{1/2}$ (at 170.2 eV) and a S $2p_{3/2}$ doublet (at approximately 168.9 eV).

The asymmetry of the C 1s core-line of polycarbazole-treated carbon fibers (sample S2) increases slightly in comparison to the untreated fiber, especially on the higher binding energy side (Fig. 4a). This may be due to the presence of N in the polycarbazole structure. The C 1s peak has been deconvoluted in four synthetic peaks. The most intense contribution

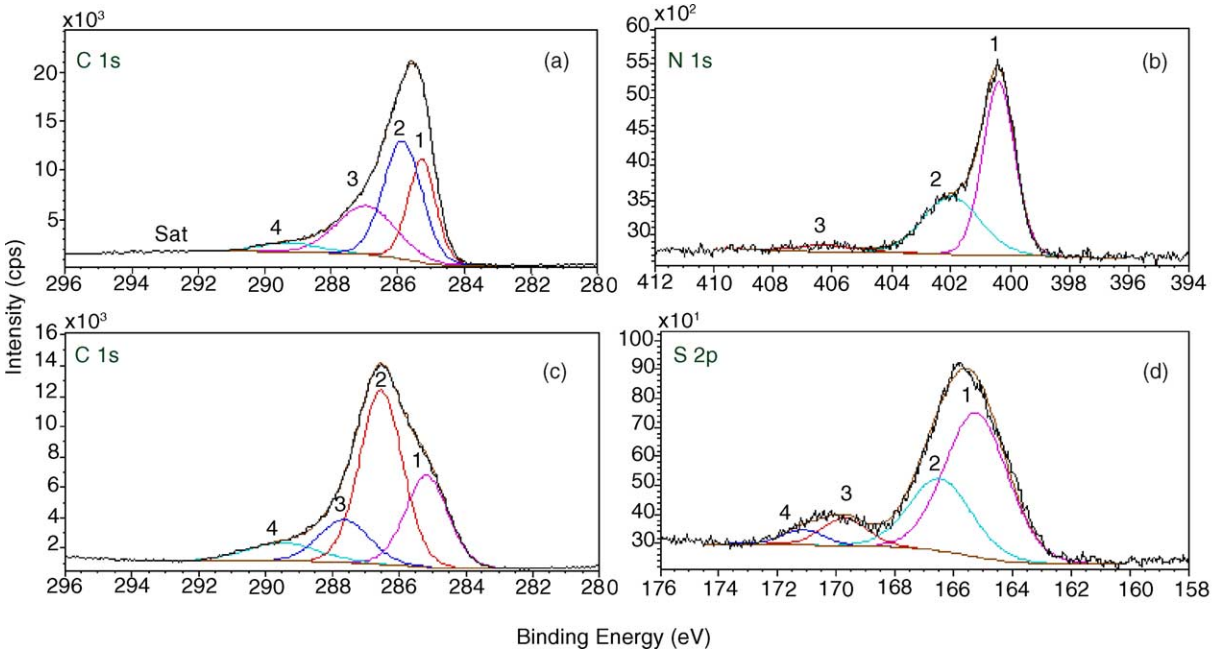

Fig. 4. Core-level XPS spectra in the region of C 1s (a); N 1s (b) for carbazole and C 1s (c) and S 2p (d) for 3-methylthiophene, on Hexcel carbon fiber.

(∼72%) has been observed from the synthetic peak 2 in Fig. 4a, which appears at approximately 0.6 eV higher binding energy than the peak 1 at 285.2 eV. The contribution of the latter is approximately 13%. The binding energy position (285.8 eV) is quite close to what is expected for N bonding in carbazole, along with a lone pair of electrons. The energy position matches closely with the database value of C 1s line for polycarbazole [14]. The rest of the synthetic peaks, denoted as 3 and 4, can be assigned to C single bonded to O and C in CO_3^{2-}/COOR functionalities, respectively.

Strong evidence of the bonding between C and N can also be found from the N 1s spectrum as shown in Fig. 4b. The narrower main peak (denoted as 1 in Fig. 4b) and the appearance of a strong shoulder at about 402.2 eV (denoted as 2) makes it completely different to the N contamination peak that has been found on the untreated carbon fibre (Fig. 3b). Another small peak is observed at approximately 406.2 eV. While the main peak can be related to N bonded to C in polycarbazole [14], the shoulder is more likely to be related to the protonated quaternary N that was present in the doping solution. The small peak denoted as 3, at somewhat higher binding energy (406.2 eV), is assigned to some form of oxygenated nitrogen based chemical composition.

In the C 1s spectrum for the methylthiophene (MeTh) treated sample (S3), the absence of any significant contribution from satellite peaks is noteworthy (Fig. 4c). XPS and UPS studies [15–17] on the electronic structures of polythiophene (polyTh), polybithiophene, polyterthiophene and poly(3-alkylthiophene) suggest a systematic evolution of the π-bonding orbital while going successively from thiophene to bithiophene and terthiophene. The work of Tourillon and Jugnet [15] suggests that for perchlorate doped and electrochemically synthesised polyTh, polybithiophene and polymethylthiophene (poly(MeTh)), the π-bonding band indicates long-range order when a polymer chain is extended up to 0.2 eV below the Fermi level. At the same time, the XPS C 1s and S 2p core-lines become broad and highly asymmetric. Broadening of the S 2p peak in doped polyTh and polybithiophene has been explained in terms of charge localisation in the oxidised polymer.

The presence of two different S-species was suggested for the doped polymers [18]. However, while studying thermochromism in alkyl-substituted polyThs, Keane and co-workers have found that shake-up features due to $\pi \rightarrow \pi^*$ transition for poly(MeTh) are high temperature phenomena. The disappearance of the shake-up structure at lower temperatures implies a stronger delocalisation of electrons [16].

The C 1s peak for the poly(MeTh) treated sample is highly skewed to the higher binding energy side, while a shoulder can also be noticed at the lower binding energy tail. In Fig. 4c the C 1s spectrum has been deconvoluted into four synthetic components: the main peak at 285.2 eV denoting C–C bonding (peak 1), a peak at 286.5 eV denoting C–S/C–O bonding (peak 2), a peak at 287.6 eV denoting C=O bonding (peak 3) and a peak at approximately 289.5 eV denoting C in CO_3/COOR (peak 4).

The S $2p_{3/2}$ peak in thiophene (Th) usually appears at approximately 164.3 eV [14]. The S in polyTh structure, however, can exist in three redox forms, although the electrical conductivity is usually assigned to only one form. The withdrawal of one electron from the polyTh molecule followed by its doping with a solution anion leads to its conducting half-oxidised polaronic state, whereas, the loss of second electron leads to the oxidised bipolaronic form. The binding energy position at 164.3 eV, however, represents the neutral form of S. In Fig. 4d, the S 2p spectra for the poly(MeTh) treated sample exhibits two broad maxima which have been deconvoluted into their $2p_{3/2}$ (peaks 1 and 3) and $2p_{1/2}$ (peaks 2 and 4) doublet structures. The $2p_{3/2}$ peak denoted as 1 in Fig. 4d appears at about 165.3 eV showing $a + 1$ eV shift from the main S $2p_{3/2}$ line. This corresponds to the +1.3 eV shift of the C peak due to C–S bonding (Fig. 4c peaks 1 and 2) and reveals a major contribution from the polaronic S, with some contributions from the S in the form of bipolaronic S/SO_4, as denoted by the doublet peaks 3 and 4.

XPS has also been used to provide a semi-quantitative insight of the effect of surface composition as a function of initial monomer feed ratio. This complements our earlier investigation of the composition by EDX against monomer feed ratio [12]. In general both the techniques show the presence of C, N and S, although, XPS provides superior surface composition results due to the greater surface sensitivity of this technique. The relative amounts of the principle elements found on the surface of the electrografted polymers under investigation are listed in Table 2.

Figs. 5 and 6 show the variation of C, O, N and S as measured by XPS analysis with the initial feed ratio of comonomers. It can be noticed from Fig. 5 that with the increase of initial feed of Cz monomer, the C content of thin film decreases, while the O content shows an increase. A similar correlation can be made between the N and S content from Fig. 6, where the N content increases in conjunction with an increase in the feed ratio, hence, an increase in the carbazole monomer content. However, as a result of the increased N content, the S content decreases, which is due to a reduced 3-methylthiophene content in the copolymer feed. On the other hand, the Cl content has almost been doubled in samples S2 to S5 for which the ratio of the $[Cz]_0/\{[Cz]_0 + [MeTh]_0$ ratio is approximately 4. This indicates a higher extent of anion doping (chlorine in perchlorate form being the doping anion).

Copolymeric composition of surface is calculated on the basis of theoretical formula of $[C_{12}NH_7] \times [C_5SH_4]_y$ Effect of initial monomer feed ratio on

Table 2
Percentage composition of C, N, S and O against the initial feed ratio of comonomers (carbazole and 3-methylthiophene) in electrografted carbon fiber surface, as measured by XPS

	Copolymer monomer	$[Cz]_0/\{[Cz]_0 + [MeTh]_0\}$	C (%)	N (%)	Cl	S (%)	O (%)
S4	MeThCz11	0.26	84.42	4.42			9.75
S5	MeThCz6	0.27	83.11	3.46	0.36	1.83	10.49
S6	MeThCz7	0.40	79.98	3.16		1.53	13.19
S7	MeThCz8	0.65	78.46	5.57	0.87	0.38	13.64
S2	Cz12	1.00	79.47	5.17	0.71	0.38	13.42
S3	MeTh13	–	71.56	2.47	1.20	2.31	17.58

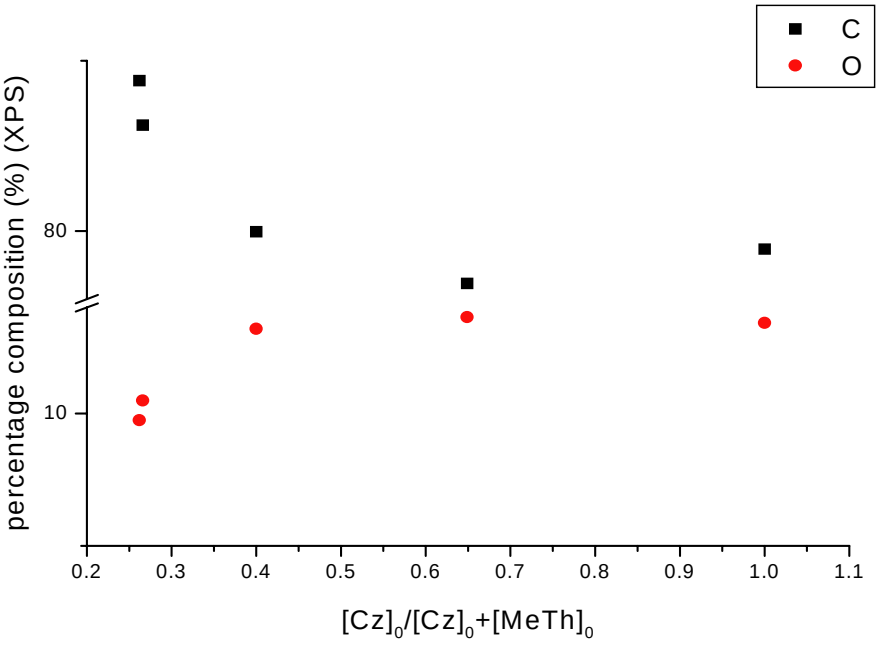

Fig. 5. Relative amount of C and O at the surface of electrografted carbon fiber as a function of initial feed ratio of carbazole and 3-methylthiophene comonomers.

the calculated x/y, and $x/(x+y)$, and the experimental results are compared in Table 3.

Since the reactivity of Cz is much higher than MeTh, resulting copolymeric structure components (block units) ratio $x/(x+y)$ was different than the initial fraction (z).

Increase in radius of grafted fiber (thickness of copolymer on the surface according to different initial

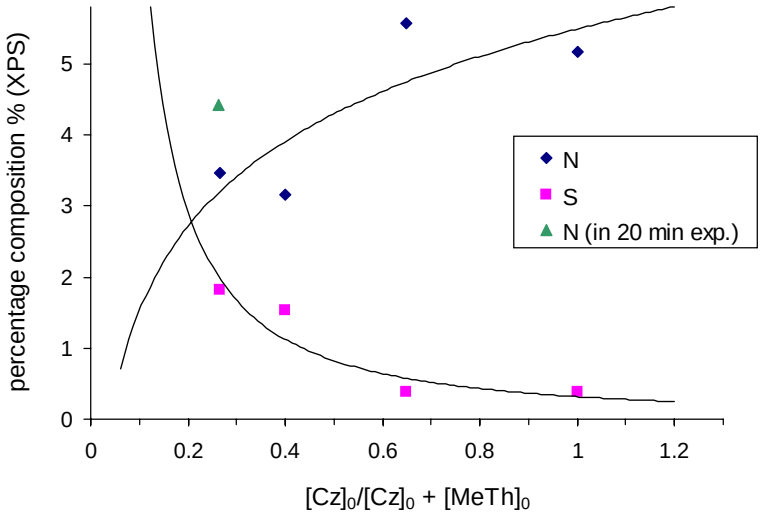

Fig. 6. Relative amount of N and S at the surface of electrografted carbon fiber as a function of initial feed ratio of carbazole and 3-methylthiophene comonomers.

Table 3
Comparison of surface composition from XPS and that calculated on the basis of theoretical formula of $[C_{12}NH_7] \times [C_5SH_4]_y$ for various initial monomer feed ratios

Fraction and feed ratio		MeThCz6 (S5) ($z = 0.27$)[a]	MeThCz7 (S6) ($z = 0.40$)[a]	MeThCz8 (S7) ($z = 0.65$)[a]	Cz12 (S2) ($z = 1.0$)[a]
From XPS[b]	N/N+S	0.654	0.674	0.936	
Calculated[c] x/y ratio for theoretical model $(CZ)_x/(MeTh)_y$		4.32	4.73	33.43	
$x/(x+y)$		0.812	0.825	0.971	1.0

[a] Fraction of initial MeTh in total $z = [Cz]_0/\{[Cz]_0 + [MeTh]_0\}$.
[b] Calculated from XPS results, impurities on the original untreated carbon fiber was not taken into account. Difference in values in some cases can be attributed to the due to difference in sensitivity and measurement depths of technique.
[c] Calculated on the basis of theoretical formula of $[C_{12}NH_7] \times [C_5SH_4]_y$.

feed ratios) versus calculated $x/(x+y)$ values (fraction of polycarbazole segments in the copolymer) were also plotted and included in the text to give more quantitative relationship between calculated and experimental results.

3.3. Raman spectroscopy

The line scans collected by Raman spectroscopy analysis (over a distance of approximately 25 μm) indicated phase homogeneity of the polymer/copolymer coatings (on the micron scale), since comparison of the resulting spectra from different areas of analysis (or on different fibers of the same composition) were practically identical.

The Raman spectrum obtained for the Hexcel carbon fiber (base material) is shown in Fig. 7. The peaks observed at both 1339.19 and 1567.45 cm^{-1} are associated with the C=C stretching and C–C aromatic bonds, respectively.

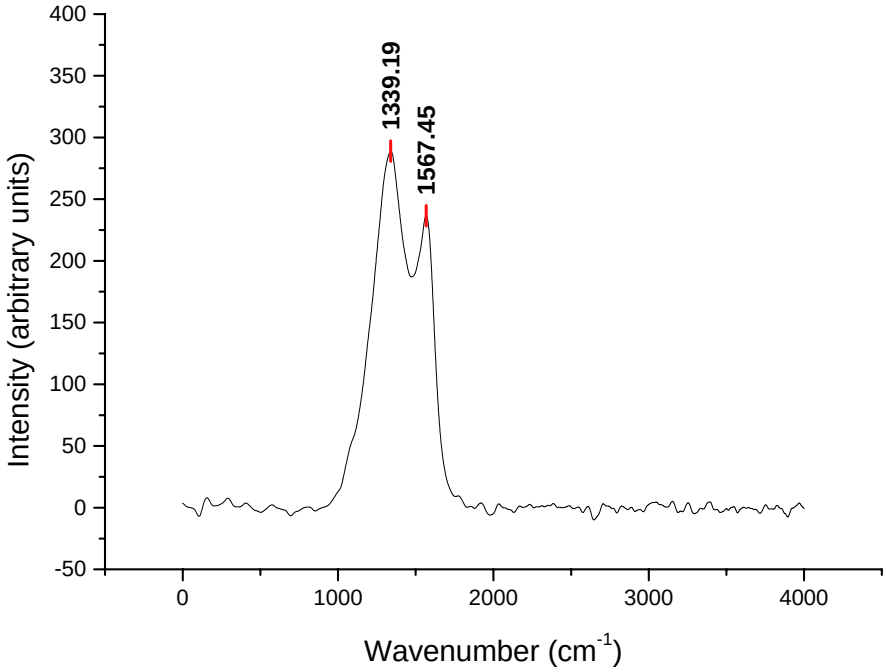

Fig. 7. Raman spectra of Hexcel carbon fiber.

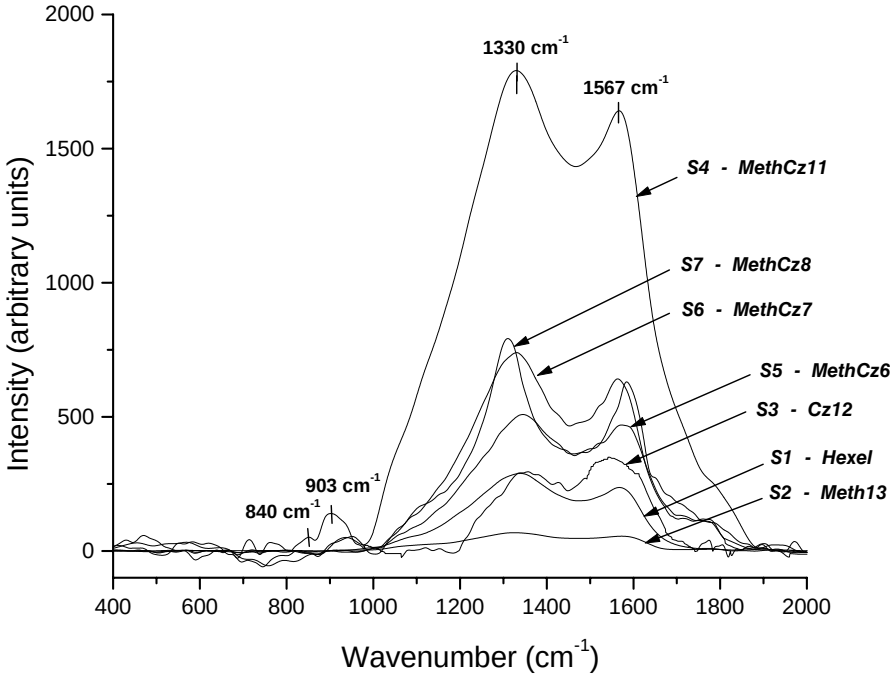

Fig. 8. Spectra obtained from sample S1–S7 (spectral range from 400 to 2000 cm^{-1}).

The spectra obtained from the samples, outlined in Table 1, are given in Fig. 8. The spectra illustrated in Fig. 8 show two major bands in the region of 1310–1345 and 1560–1585 cm^{-1}, which are again related to stretching of various carbon bonds. The later peak is related to the γ(C–C) ring at 1583–1599 cm^{-1} (assigned to aromatic ring of carbazole unit of copolymer) and the former peak at approximately 1330 cm^{-1} corresponds with the γ(C=C) ring assignment. The various stretching assignments and their related bands are given in Table 4. Results obtained from intensive Raman spectroscopy work conducted by Pulay and co-workers [19–21] and Hernadez et al. [22] on thiophene and 3-methylthiophene is in agreement with results given in this paper and with previous FTIR-ATR results [12].Pellegrino et al. [23] also mentions that C–S–C bond stretching should have a band at approximately 840 cm^{-1} as indicated as a weak Raman shift by samples with high sulphur content (i.e., samples S3–S7).

Bands in the region of 840–970 cm^{-1} are due to the substituted aromatic ring in carbazole and to the in plane deformation of the –C–H bonds [4]. The band that should be observed in sample S2 at approximately 900 cm^{-1} is related to the C–N stretching mode and ring vibration of carbazole rings [24]. However, this band was only observed in sample S7, which has high N content according to XPS.

In this paper, many bond interactions related to carbazole should be observed, especially in the region

Table 4
Principle Raman spectra assignments and frequencies observed for electrografted copolymers on carbon fiber with respect to different composition of functional groups of copolymers and of electrografted fiber surface

Sample number	Wavenumbers γ(C=C) ring	α(C–C) Ring (cm^{-1})
S1, untreated CF	1339.19	1567.45
S2, [Cz12 (aromatic ring)]	1356.50	1541.23
S3, (MeTh13)	1316.73	1578.4
S4, (MeThCz11)	1329.94	1566.74
S5, (MeTh-Cz6)	1344.67	1571.80
S6, (MeThCz7)	1331.00	1563.96
S7, (MeThCz8)	1309.81	1584.18

γ Represents stretching.

of 1000–1200 cm^{-1} [25]. The identification of the exact position of the Raman shift is impossible to differentiate, even if deconvolution routines are applied. However, the presence of slight shoulders on the principle bands can be used to provide a tentative guess towards what may be occurring in these conductive copolymer samples. Possible bond interactions related to in plane C–H bending modes and phenyl group ''ring breathing'' modes could be observable, which has been reported in other investigations into carbazole-based polymers [25].

Shoulders observed at approximately 1225 cm^{-1} could be related to C–O bond stretching mode of the carboxyl acid dimer, which could explain the downshift (of almost 40 cm^{-1}) in the C=C stretching band (present in the region of 1310–1345 cm^{-1}) as carbazole substitution is carried out. A similar result was observed by Lao et al. [25], in their study of substituted carbazole-based derivatives.

Shoulders observed in the region of 1230–1235 cm^{-1} in polycarbazole homopolymer (Cz12) and copolymers corresponds to the stretching vibration of γ(C–N). Casado et al. [26] deliberates that a down shift of the band at approximately 1330 cm^{-1} can be indicative of charge defects that can in fact be extending from the phenyl caps.

The principle band for a mono-substituted carbazole should be present at approximately 1290 cm^{-1} [25].

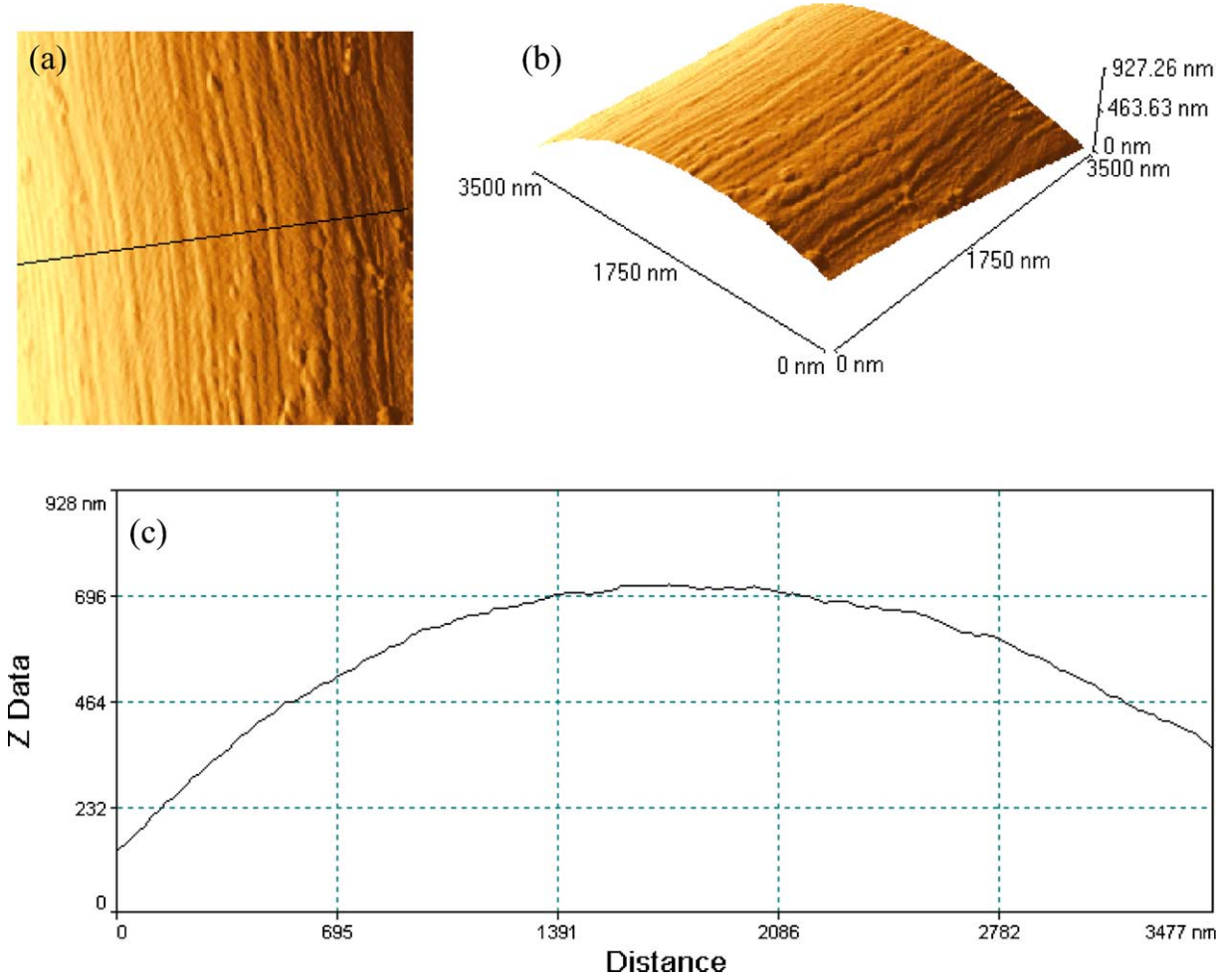

Fig. 9. (a) Represents a 2D image of the uncoated Hexcel carbon fiber (S-1); (b) represent a 3D image of the same surface and (c) is the line analysis related to the black line in image (a).

This band is associated with $C_2 > N–H$ bond vibrations. Hence, the substitution of the 1 or 8 position of the carbazole polymer network results in a weakening of the C–C bonds of the carbazole network. This results in an up shift in band position relating to the C–C bridge bonds of the phenyl rings becoming the more intense Raman shift, as observed in results obtained in this paper.

Zarbin et al. [27] have shown that the principle bands for a similar copolymer appear at 1317 and 1561 cm^{-1} and are representative of C=C and C−C stretching, respectively, which is also an accepted observation from other published studies [28–33]. This is assignable to stretching of the phenyl end caps [26] and it is strongly related to the π–π^* transition, directly related to the distribution of conjugation lengths [34] which was previously deliberated in the XPS section of this paper. The Raman frequencies in this region are the most interesting for these copolymer samples as it indicates the activeness of their carbon-based bonds.

The investigation of quinquethiophene [35] illustrates similar stretching modes in the thiophene rings to results obtained from these copolymer samples. Bosisio et al. [35] further deliberates that the band positions and their widths are consistent with the molecular excitation model of the conductive copolymers.

The broadness of the Raman shifts observed in the region of 1200–1600 cm^{-1} are attributed to the overlap of the other possible bond attributions, such as, C–N stretching and C–H bending [27]. Other band positions at approximately 1080, 1050, 980 and 940 cm^{-1}, although weak in intensity, should also be observed indicating the bending of C–H based bonds. However, small and weak Raman shifts are only observed for samples S2 and S4–S7.

Cravino et al. [36] describes that the high intensity of the Raman shifts in combination with broad bands can be indicative of a high dislocation along the network chains of the copolymer. The intensities of the principle band positions increase as a function of feed ratio of 3-methylthiophene and carbazole. This was observed in previous FTIRATR results on similar materials [12]. Lao et al. [25] describes that N–H stretching in the region of 1400 and 1630 cm^{-1} may result in an increase in the observed intensity of these bands in the Raman spectra. This concept is consistent with XPS results as the N and H contents increase, so do the intensity of the bands in this region.

Catellani et al. [34] (1996) describes the downshift of the principle band (related to C=C stretching) at approximately 1320 cm^{-1} (by approximately 50 cm^{-1}) as being associated with the substitution of an alkyl chain present in the thiophene network with a hydrogen atom, which may lead to increase C=C stretching frequencies. This could explain the downshift and the increase in intensity of the principle bands as the feed ratio of 3-methylthiophene-carbazole copolymer is increased (increased H content). The very weak band present at approximately 1455 cm^{-1} in the

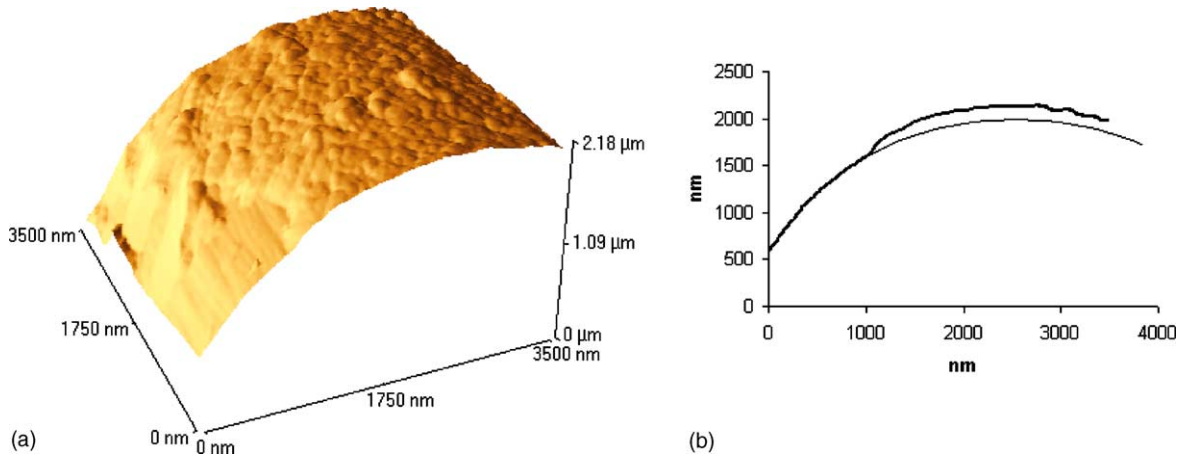

Fig. 10. (a) 3D AFM image of sample S-2 z11); (b) thick line: line analysis in the position indicated by the arrow in (a); (b) thin line: sketch of the carbon fiber surface underneath the coating.

carbazole spectra only (sample S2) is attributed to synergistic vibration of the carbazole ring [37].

3.4. AFM results of electrografted copolymeric structure on the carbon fiber surface

AFM images of carbon fiber were obtained by fixing the fiber on a piece of silicon wafer with resin, as described in the experimental section. The AFM measurement was then performed by positioning the scanner on the top of the carbon fiber itself. The size of the area was selected in order that the AFM tip could remain on the top of the fiber during the measurement. This set-up produced curved images representing the curved portion of the fiber analysed.

Fig. 9 shows an AFM image of the uncoated Hexcel carbon fiber. Narrow grooves, channels or striatures, due to the structure of the carbon fiber are characteristic of the surface. The striatures are generated by alignment of carbon atoms rings regularly lined up along the longitudinal direction of a fiber.

Fig. 10 shows the carbon surface modified by carbazole electropolymerization. The Cz polymer only partly covers the carbon fiber surface. The area pointed to by the arrow shows a region in which the coating is absent, and the striatures of the uncoated surface are similar to the one imaged in Fig. 9. Fig. 10a shows that the top of the fiber is coated by the Cz polymer and from the line analysis in Fig. 10b, the thickness of the coating can be estimated to be about 150 nm.

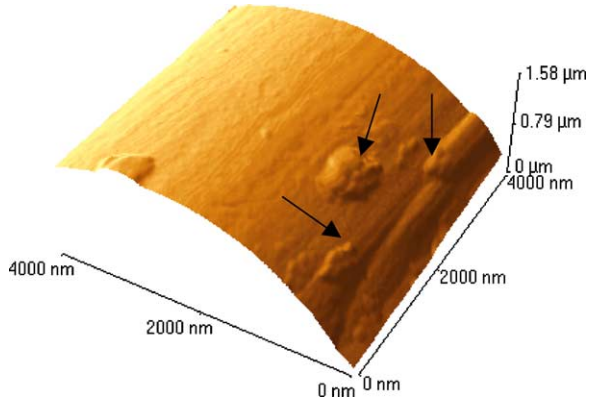

Fig. 11. 3D AFM image of sample S-3 (MeTh13).

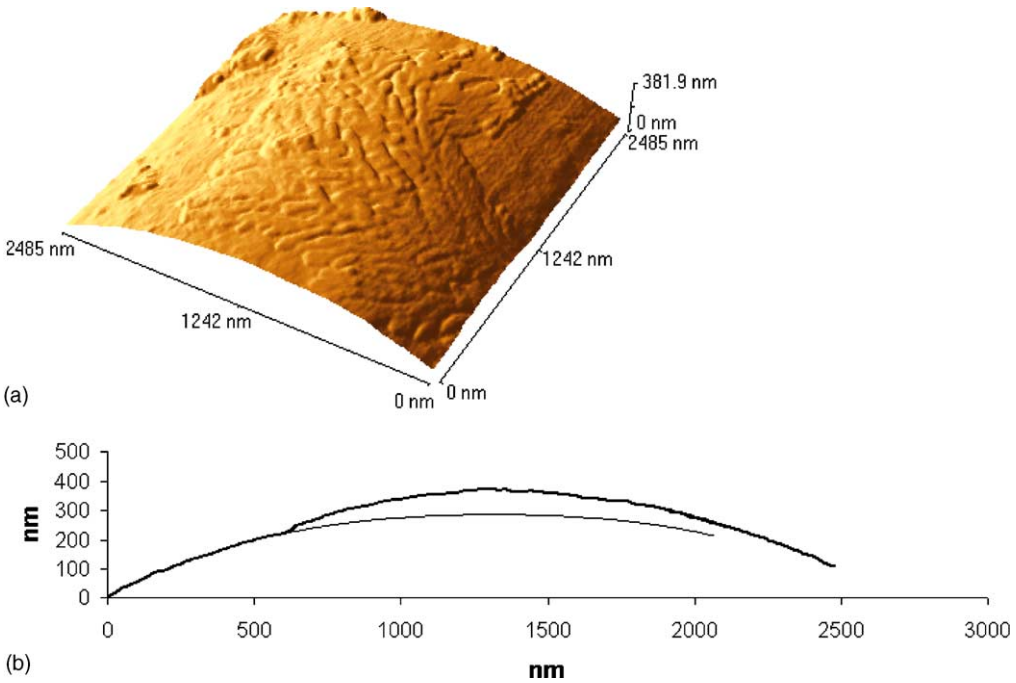

Fig. 12. (a) 3D AFM image of sample S-3 (MeTh13); (b) thick line: line analysis in the position indicated by the arrow in (a); (b) thin line: sketch of the carbon fiber surface underneath the coating.

The coating is shaped in form of grains with average radius of 150 nm, (measured by using the line analysis on the SPM software). Considering the maximum length of the Cz monomer being 8.6 Å, (Cerius^2 Molecular Modelling Software), the number of monomers that form the strand in a grain can be calculated as 170.

AFM analysis of sample S3 was conducted on various fibers in different areas. The analysis shows that electrografting of poly(MeTh) on Hexcel carbon fiber produce a very thin film as can be verified by comparing Figs. 9 and 11. From these figures, it is possible to observe that the striatures of the uncoated fiber are less clear after electrografting of poly(MeTh), due to thin film coating.

Near steps or defects on the carbon fiber surface, the polymer typically grows forming grains (arrows in Fig. 12). Fig. 12a shows an area in which proliferation of grains, from the bottom right of the image, produces a fractal structure that expands along the carbon fiber surface. From line analysis in Fig. 12b, the thickness of the partial coating is estimated at about 100 nm. The maximum length of the monomer of 3-MeTh was calculated using Cerius^2 Molecular Modelling Software as 5.2 Å. The average radius of a grain measured from the line analysis on the AFM image in Fig. 12 is 70 nm, which suggests that about 130 monomer units form the polymer strand in each grain. From another point of view, if the thickness of two layers of 4[αT] (unsubstituted tetrathiophene-octomer) is given as

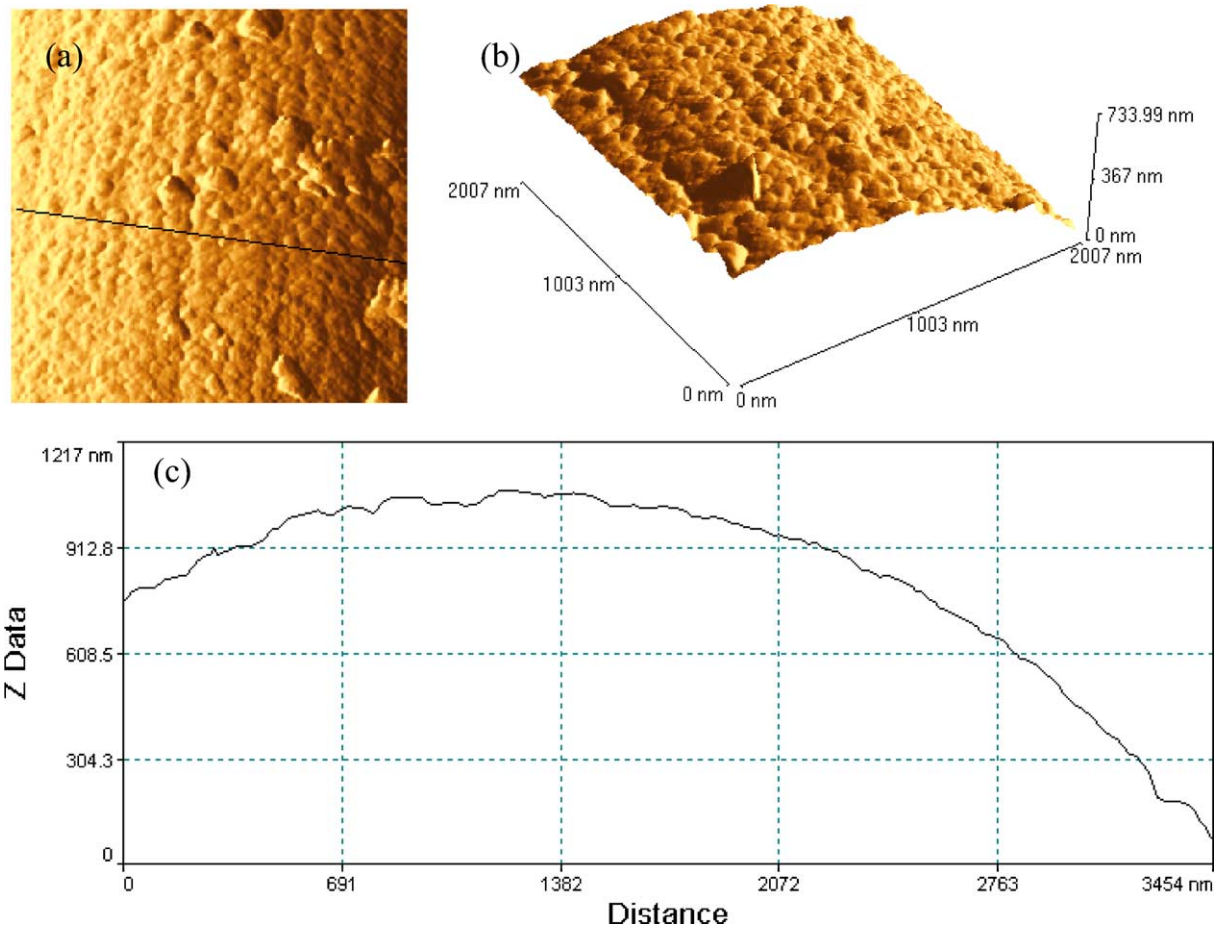

Fig. 13. (a) Represents a 2D image of sample S4; (b) represent a 3D image of the same surface and (c) is the line analysis related to the black line in image (a).

~15.3 Å, a 49 octomer of 3-MeTh units chain, with molecular weight of ~37000, could form each grain electrografted on the surface.

X-ray diffraction studies have been published in relationship to the crystallinity of powder or thin films of polythiophene. Two conformations of polthiophenes are possible: a linear and nearly planar all trans structure (rod conformation) and a helical all-cis one (coil conformation). These geometries are separated by an energy barrier of about 3–6 kcal/mol. [38–40]. From AFM images in Fig. 12, it is suggested that 3-MeTh electrocoating could have an amorphous structure on the thin-coated part of the fiber and have a crystalline structure on the thick-coated part, where grains are present, even if at the moment we do not have any experimental evidence of this.

Fig. 13 shows the AFM image of sample S4. In this case, a Cz-MeTh copolymer (with a feed ratio 0.27) was electropolymerised onto the carbon fiber surface, by constant current electrolysis, for 20 min. The surface of carbon fiber is totally and homogeneously coated by the copolymer. The average radius of the grains is measured at approximately 80 nm. This radius is in between the radius of the grains of the two monomers and can be due to the combined copolymerisation of the two monomers.

Fig. 14 shows the AFM image of sample S6. The feed ratio of electropolymerisation was in this case

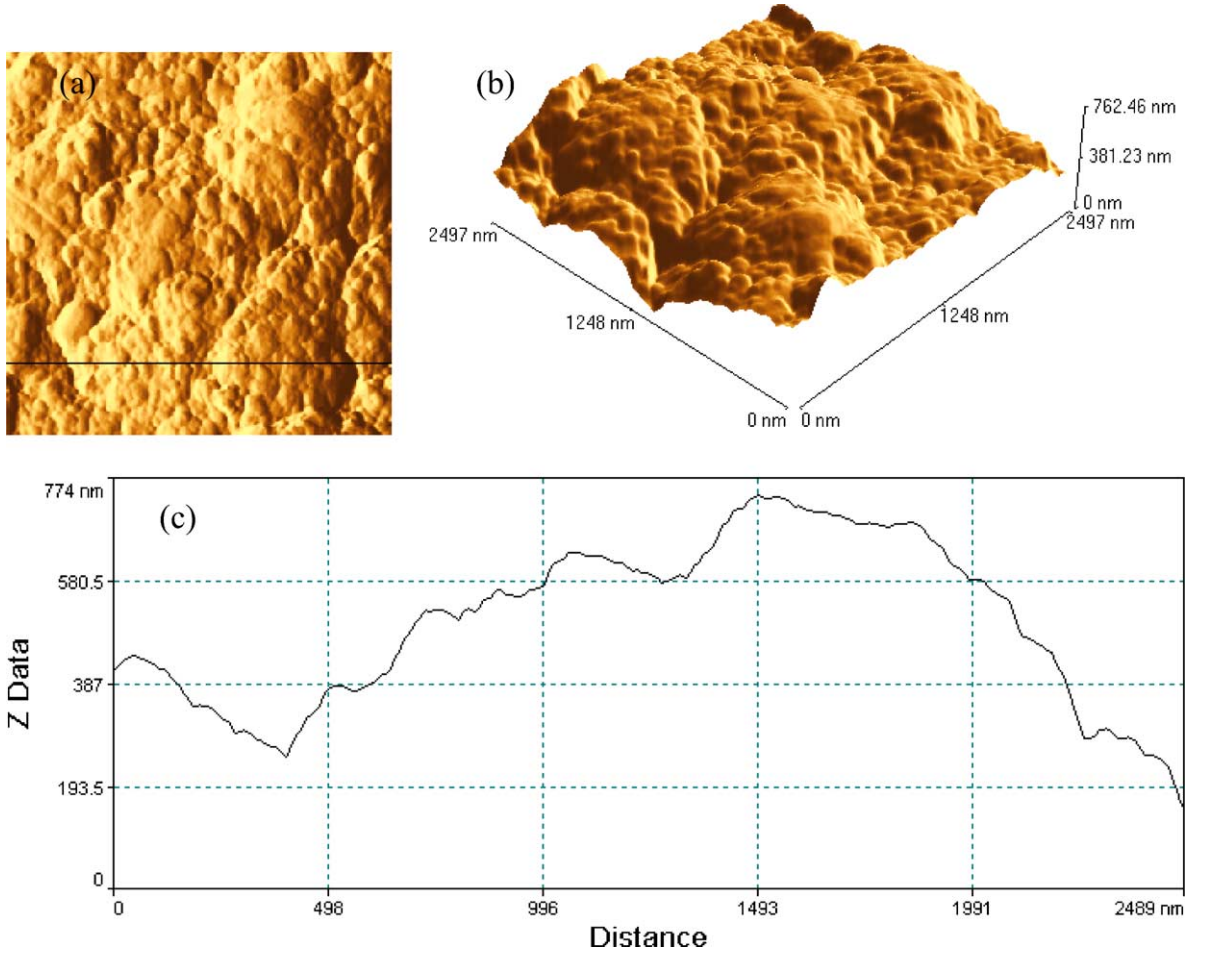

Fig. 14. (a) Represents a 2D image of sample S6; (b) represents a 3D image of the same surface and (c) is the line analysis related to the black line in image (a).

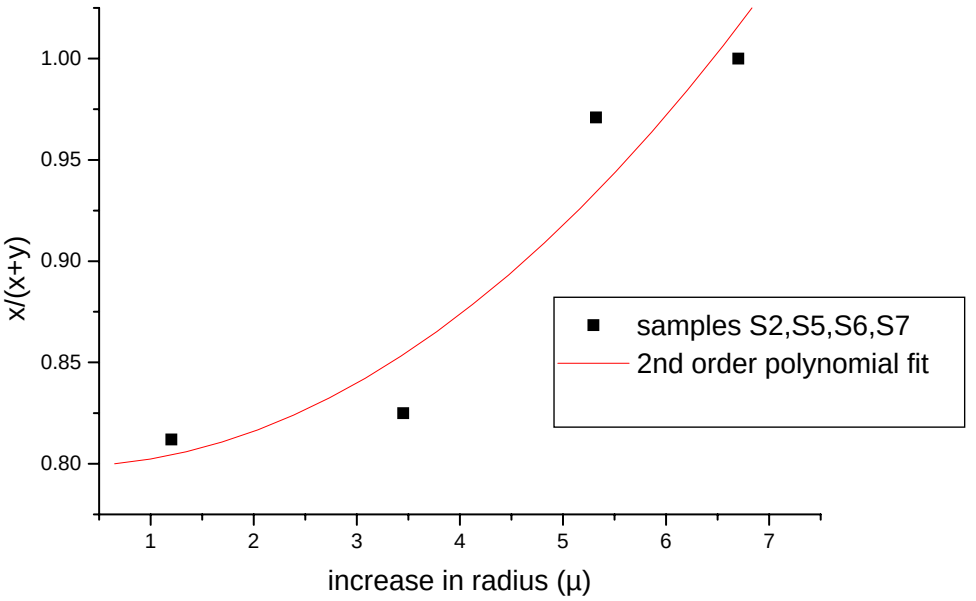

Fig. 15. The calculated $x/(x+y)$ values (fraction of polycarbazole segments in the copolymer) as a function of the increase in the radius of grafted fiber (thickness of copolymer on the surface according to different initial feed ratios). The trend follows a second order polynomial relation with a R^2 value of 0.92. The coefficients of the polynomial are (A) 0.799; (B) −0.0016; (C) 0.0051.

0.66, with a larger percentage of 3-MeTh. The polymerisation time was 120 min. The carbon fiber surface appears completely covered. The coating is not homogeneous and presents a multilayer structure that suggests overlapping of layers of copolymer during the prolonged time of electrolysis. The average radius of the grains is, in this case, about 50 nm. With a multilayer structure thickness of 485 nm (Fig. 14c), the surface is rough due to random agglomeration of at least 10 layers of polymer. The grains in this multilayer configuration have a radius of about 1 μm.

By modelling of a unit of copolymer (using Cerius[2] Molecular Modelling Software), i.e., the maximum length of the cooligomeric unit of sample S6 [where *x*/*y* (Cz/MeTh) ratio found to be about 5/1 from XPS results] was found to be 42.8 Å. Calculation of number of units of coligomeric structure of $(Cz)_5(MeTh)_1$ shows that the average radius of grains compose of 12 $[Cz]_5[MeTh]_1$ units (molecular weight of ∼11,000). Similar calculations for a multiplayer structure corresponds to the chain of 114 $[Cz]_5[MeTh]_1$ units (Molecular weight of ∼105,000) which was electrografted on the surface of carbon fiber.

If the polymer strands were formed from the same number of copolymer chains, the grains should have been larger for sample S6 than for sample S4. This is not the case and it is supposed that the copolymerisation ratio between Cz and MeTh does not follow the feed ratio of the starting solution.

Additionally Fig. 15 indicates the second order polynomial relationship between increase in radius of grafted fiber (thickness of copolymer on the surface according to different initial feed ratios) against calculated $x/(x+y)$ values (fraction of polycarbazole segments in the copolymer).

4. Conclusions

The characterisation of electrodeposited copolymeric thin films on a carbon fiber surface, by means of surface composition (XPS), morphological (AFM), and functionality of the conjugated system (Raman spectrometric method), was performed as a function of the initial feed ratio of comonomers, which are used for the formation of thin films (nanosize films).

The surface composition, as revealed from the XPS study, showed the evidence of C–N bonding in the case of Cz coated fibers and C–S bonding in the case of 3-Meth coated fibers. For the fibers coated with

copolymers, the presence of both the C–S and C–N bonding was identified. In general, the O, N and Cl contents showed an increase as a function of increasing comonomer feed ratio, while the S content demonstrated a decrease.

AFM is a useful tool for the analysis of electrografted carbon fibers. In the analysis carried out in this work, it has been shown that both Cz and MeTh can polymerize onto the carbon fiber surface when present alone in solution, but in these cases the coating is not homogeneous and part of the carbon fiber surface remains uncoated. When the two monomers are present simultaneously in the starting solution, they copolymerise producing a full covering of the carbon fiber surface. Depending on the electropolymerisation time, the coating can be homogeneous or with a highly rough multilayered structure. Hence, the strength of the carbon fiber composites strongly relates to the presence and types of such interfacial functional conjugated systems, which are easily formed on the surface of carbon fibers.

From Raman spectroscopy, phase homogeneity of the polymer/copolymer coatings was observed and the typical stretching and deformation assignments and their related bands for both carbazole and 3-methylthiophene were also identified. The identification of the exact position of certain less dominant Raman shifts was difficult to differentiate. However, the presence of shoulders on the principle bands was used to provide conclusions as to what vibrational modes were present in these conductive copolymer samples. The broad band nature of the Raman shifts observed in the collected spectra were thought to be indicative of a high dislocation along the network chains of the copolymer, resulting in overlapping spectra from both the carbon fiber and the copolymer coatings.

References

[1] J.O. Iroh, K.M.S. Jordan, Surf. Eng. 16 (2000) 303.
[2] J.-M. Park, Y.-M. Kim, D.-J. Yoon, J. Colloid Interface Sci. 231 (2000) 114.
[3] H. Ishida, Controlled Interphases in Composite Materials, Elsevier, New York, 1990.
[4] A.S. Sarac, A. Bismarck, E. Kumru, J. Springer, Synth. Met. 123 (2001) 411–423.
[5] E. Kumru, J. Springer, A.S. Sarac, A. Bismarck, Synth. Met. 123 (2001) 391–402.
[6] E. Sezer, A.S. Sarac, Int. J. Polym. Mater. (2003), in press.
[7] A. Bismarck, A. Menner, J. Barner, A.F. Lee, K. Wilson, J. Springer, J.P. Rabe, A.S. Sarac, Surf. Coat. Technol. 145 (2001) 164–175.
[8] A. Bismarck, A. Menner, E. Kumru, A.S. Sarac, M. Bistriz, E. Shulz, J. Mater. Sci. 37 (3) (2002) 461–471.
[9] A.S. Sarac, G. Sönmez, F.Ç. Cebeci, J. Appl. Electrochem. 33 (3–4) (2003) 295–301.
[10] E. Sezer, M. Van Hooren, A.S. Sarac, M.L. Hallensleben, J. Polym. Sci. A Polym. Chem. 37 (1999) 379–381.
[11] G.A. Sotzing, J.R. Reynolds, P.J. Steel, Chem. Mater. 8 (1996) 882–889.
[12] A.S. Sarac, J. Springer, Surf. Coat. Tech.160 (2002) 227–238.
[13] D. Briggs, M.P. Seah (Eds.), Practical Surface Analysis: V1, Auger and X-ray Photoelectron Spectroscopy, Wiley, Chichester, 1990.
[14] NIST Database, version 3.1, 2001.
[15] G. Tourillon, Y. Jugnet, J. Chem. Phys. 89 (1988) 195.
[16] M.P. Keane, S. Svensson, A. Navesde Brito, N. Correia, S. Lunell, B. Sjogren, O. Iganäs, W.R. Salaneck, J. Chem. Phys. 93 (1990) 6357.
[17] C.R. Wu, J.O. Nilsson, O. Iganäs, W.R. Salaneck, J.E. Österholm, J.L. Brédas, Synth. Met. 21 (1987) 197.
[18] G. Morea, L. Sabbatini, P.G. Zambonin, A.J. Swift, R.H. West, J.C. Vickerman, Macromolecules 24 (1991) 3630.
[19] P. Pulay, G. Fogarasi, G. Pang, J.E. Boggs, J. Am. Cer. Soc. 101 (1979) 2550.
[20] P. Pulay, G. Fogarasi, J.E. Boggs, J. Chem. Phys. 74 (1981) 3999.
[21] G. Rauhut, P. Pulay, J. Phys. Chem. 99 (1995) 3093.
[22] V. Hernadez, F.J. Ramirez, J. Casado, J.T. Lopez Navarrette, J. Phys. Chem. 100 (1996) 2907.
[23] O. Pellegrino, M.R. Vilar, G. Horowitz, F. Kouki, F. Garnier, Thin Solid Films 327-329 (1998) 252–255.
[24] D. Lin-Vein, N.B. Colthup, W.G. Fateley, L.G. Grasselli, The Handbook of Infrared and Raman Characteristic Frequencies of Organic Molecules, Academic press, San Diego, 1991.
[25] W. Lao, X. Chuanzhi, J. Shengfu, Y. Jinmao, O. Qingyu, Spectrochimica Acta A 56 (2000) 2049–2060.
[26] J. Casado, V. Hernandez, S. Hotta, J.T. Lopez Navarrette, Synth. Met. 119 (2001) 305–306.
[27] A.J.G. Zarbin, M.A. De Paoli, O.L. Alves, Synth. Met. 99 (1999) 227–235.
[28] R. Kostic, D. Racovic, S.A. Stepanyan, J.E. Davidova, L.A. Gribov, J. Chem. Phys. 102 (1995) 3104.
[29] S.P. Armes, Synth. Met. 20 (1987) 365.
[30] S. Rapi, V. Bocchi, G.P. Gardini, Synth. Met. 24 (3) (1988) 217–221.
[31] G. Louran, J.Y. Mevellec, S. Lefrant, J.P. Buisson, D. Fichou, M.P. Teulade-Fichou, Synth. Met. 69 (1995) 351–352.
[32] F.R. Dollish, W.G. Fateley, F.F. Bentley, Characteristic Raman Frequencies of Organic Compounds, Wiley, US, 1974.
[33] T. Kupka, R. Wrzalik, G. Pasterna, K. Pasterny, J. Mol. Struct. 616 (2002) 17–32.

[34] M. Catellani, S. Luzzati, R. Mendichi, A.G. Schieroni, P.C. Stein, Polymer 7 (1996) 1059–1064.
[35] R. Bosisio, C. Botta, A. Colombo, S. Destri, W. Porzio, E. Grilli, R. Turbino, G. Bongiovanni, A. Mura, G. Di Silvesro, Synth. Met. 87 (1997) 23–29.
[36] A. Cravino, H. Neugebauer, N.S. Sariciftci, M. Catallani, S. Luzzati, (2003), in press.
[37] M. Tamada, H. Koshikawa, H. Omichi, Thin Solid Films 293 (1997) 113–116.
[38] Z. Mo, K.B. Lee, Y.B. Moon, M. Kobayashi, A.J. Heeger, F. Wudl, Macromolecules 18 (1985) 1972.
[39] F. Garnier, G. Tourillon, Y. Barraud, H. Dexpert, J. Mater. Sci. 20 (1985) 2687.
[40] D. Fischou, J. Mater. Chem. 10 (2000) 571.